Korean J. of Chem. Eng., 13(3), 234-241 (1996)

MASS TRANSFER IN A COUNTERCURRENT SPRAY COLUMN AT SUPERCRITICAL CONDITIONS

Byung-Soo Chun†, Hwae-Geon Lee*, Jae-Kee Cheon* and Gordon Wilkinson**

Department of Food Engineering, Pusan National University of Technology
*Department of Chemical Engineering, Pusan National University of Technology, Korea
**School of Chemical Technology, University of South Australia, The Levels S.A.5095
(Received 24 May 1995 • accepted 29 February 1996)

Abstract – Mass transfer characteristics were determined for countercurrent extraction in a spray column with supercritical carbon dioxide solvent. Feeds were 5 and 10 vol% aqueous ethanol and iso-propanol at 25-65°C and 6.89-15.51 MPa. Results obtained in a 22 mm inside diameter column showed enhanced extraction efficiencies over comparable liquid-liquid systems. The models based on conventional liquid-liquid extraction were modified to correlate overall mass transfer coefficients for supercritical conditions. The constant value in the model of measuring individual mass transfer coefficient was influenced by the density of carbon dioxide and the system used.

Key words: Mass Transfer, Spray Column, Supercritical Carbon Dioxide, Hold-up, Drop Size

INTRODUCTION

Despite their poor efficiency, Spray columns have long been used for research on chemical separation processes such as, liquid extraction, gas absorption, stripping and distillation because of their simple geometry and the ability to define more clearly some of the system characteristics such as interfacial area.

Liquid-liquid extraction [Pratt, 1955] is performed by continuously contacting two immiscible liquids, one of which contains the desired component. The operation involves three steps namely, 1) contacting, 2) extraction and 3) solvent recovery. The "heavier" (more dense) liquid enters at the top of the column and flows countercurrent to the lighter liquid entering at the bottom. Frequently, as in this case, the continuous phase is heavier, and the lighter is the dispersed phase which enters the column via a distributor which in turn produces droplets and so disperses the phase.

Supercritical fluid extraction is a separation technique broadly similar to that of liquid-liquid extraction, but with some notable differences, for instance it has characteristics similar to gas absorption, such as a larger density difference between the phases yet the density of the supercritical phase gives it liquid-like solubilities. In studying mass transfer, it was essential to consider several factors. These included drop size, interfacial area, hold-up of the dispersed phase, solute distribution coefficient and interfacial tension, all of which have an effect on the mass transfer.

For conventional liquid-liquid extraction there have been many studies using the spray column [Ruby and Elgin, 1955; Thornton, 1992]. In recent years interest has turned to supercritical extraction, but few papers have been published on the hydrodynamics and mass transfer behaviour of such systems in continuous countercurrent extraction columns.

Brunner and Kreim [1986] studied mass transfer in the extraction of ethanol from aqueous streams as a function of pressure, temperature and the ratio between solvent and feed in a spray column with carbon dioxide under supercritical conditions. It was reported in his work that the mass transfer rate increased by a factor of ten, compared with that of conventional liquid-liquid extraction.

Lahiere and Fair [1987], and Rathkamp et al. [1987] studied mass transfer and hydrodynamic characteristics in a 25.4 mm diameter spray column, using supercritical carbon dioxide solvent. Ethanol and iso-propanol were each extracted with dense phase carbon dioxide at temperatures of 25-40°C and pressures 8.27-10.34 MPa. In agreement with Brunner, extraction efficiency up to ten times of that of normal liquid extraction was obtained for the supercritical system.

The purpose of this work was to study whether mass transfer in supercritical fluid extraction was more like liquid-liquid extraction, gas absorption or perhaps even distillation and to obtain fundamental mass transfer data needed for the design of supercritical fluid extraction columns and to investigate packed column hydrodynamic behaviour under supercritical conditions.

THEORY

Mass transfer takes place during contact of the two immiscible phases. Perhaps the most useful concept in liquid extraction and gas absorption is the two-film theory of Whitman [1923] in which solute concentration in the bulk (or continuous) phase is presumed uniform (due to convection currents) and concentration differences are neglected, except in the vicinity of the interface.

Assuming that there is equilibrium at the interface and that there are stagnant (ie non-convective) films on each side of the interface, then the molar mass flux of solute (mol/s·m^2) across the interface may be expressed as

$$Na = K_{oc}\,a\,(X^* - X) = K_{od}\,a\,(Y - Y^*) \quad (1)$$

†To whom all correspondences should be addressed.

The interfacial area, a (m^2/m^3), can be estimated from the following Eq. (2) assuming that the dispersed phase droplets are spherical. ϕ_d refers to the dispersed phase hold-up and ε is the volume fraction of the dispersed phase in the extraction zone at any instant.

$$a=\frac{6\varepsilon\phi_d}{d_s} \tag{2}$$

In this equation drop diameter d_s is calculated as the Sauter mean drop diameter to allow for minor departures from sphericity. The overall mass transfer coefficient can be expressed in terms of the individual film coefficients for the continuous phase in the following manner:

$$\frac{1}{K_{oc}}=\frac{1}{k_c}+\frac{1}{m_s k_d} \tag{3}$$

In a spray column, four distinct stages of mass transfer can be recognised. First, when the dispersed phase enters through the distributor, mass transfer occurs due to the creation of a new interfacial area as the drops form [Skelland and Huang, 1979]. Mass transfer in the first stage was neglected because the total amount of solute transferred was very small.

The second stage is when the dense phase carbon dioxide stream breaks up into droplets by interfacial forces. Mass transfer again occurs due to the creation of a new surface. Higbie [1935] developed a model to estimate individual mass transfer coefficients.

Third, as the droplets travel up through the continuous phase in the column to the interface at the top, most of the mass transfer takes place. The mass transfer from the rising drops depends on several factors which include drop size, hold-up, slip velocity, interfacial tension, time of contact, drop hydrodynamics (such as internal circulation) interfacial waves and any drop oscillation.

The final stage occurs when the droplets coalesce at the interface at the end of their passage through the column. A small amount of mass transfer also occurs here [Johnson and Hamielec, 1960]. Drop formation mass transfer was approximately ten times greater than during drop coalescence [Treybal, 1980]. This was explained by the intense internal convection at the interface during drop formation.

In this work, to provide a basis for the correlation of individual mass transfer coefficients k_c and k_d in the third stage, a dimensional analysis was performed. For the continuous phase this gave:

$$\frac{k_c d_s}{D_c}\propto f\left(\frac{V_s\rho_c d_s}{\mu_c},\ \frac{\mu_c}{\rho_c D_c},\ \frac{d_s^2\rho_c g}{\gamma}\ \cdots\right) \tag{4}$$

and for the dispersed phase :

$$k_d \propto f(\text{density, viscosity, diffusivity, slip velocity}) \tag{5}$$

For a differential contactor, column height H can be expressed in terms of the height of a transfer unit HTU_{oc}, and the number of transfer units NTU_{oc}. Based on the continuous phase:

$$H=[HTU][NTU]=\frac{V_c}{K_{oc}a}\int_{x_1}^{x_2}\frac{dx}{x-x^*} \tag{6}$$

At the normal conditions of room temperature and 0.103 MPa, the solvent carbon dioxide and carrier water are substantially immiscible. However, at high pressure, the solubility of water into the carbon dioxide may be significant and needs to be considered. Near the critical point, the solubility of water in carbon dioxide is under 2 mol% and can be neglected so that the distribution curve is substantially straight. Henry's law can therefore apply, and the NTU_{oc} is given by the following equation:

$$NTU_{oc}=\frac{\ln\left[\left\{\frac{X_{c,in}-(X_{d,in}/m_s)}{X_{c,out}-(X_{d,in}/m_s)}\right\}\left(1-\frac{1}{\beta}\right)+\frac{1}{\beta}\right]}{[1-(1/\beta)]} \tag{7}$$

where $\beta=(\rho_d V_d m_s)/(\rho_d V_c)$

The height equivalent to a theoretical stage is defined as

$$HETS=\frac{\beta(\ln\beta)(HTU)}{\beta-1} \tag{8}$$

$$\text{if}\ \frac{V_d m_s}{V_c}=1,\ \text{then HETS}=\text{HTU} \tag{9}$$

EXPERIMENTAL

1. Apparatus

Fig. 1 shows the flow diagram of the countercurrent spray column. The column consisted of a 22.7 mm i.d. tube extraction column equipped with view cells at each end. Column length, from distributor to interface, was 867 mm. The dispersed phase distributor consisted of a capped tube perforated with eight, 1.6 mm dia holes equidistant near the circumference.

The column temperature was maintained constant by a controlled-temperature air chamber. In-line filters were installed in all flow lines to prevent blockages, specifically up-stream of the sampling and metering valves. Pressure relief valves guarded against inadvertent over-pressure at the pump outlet, and of the column.

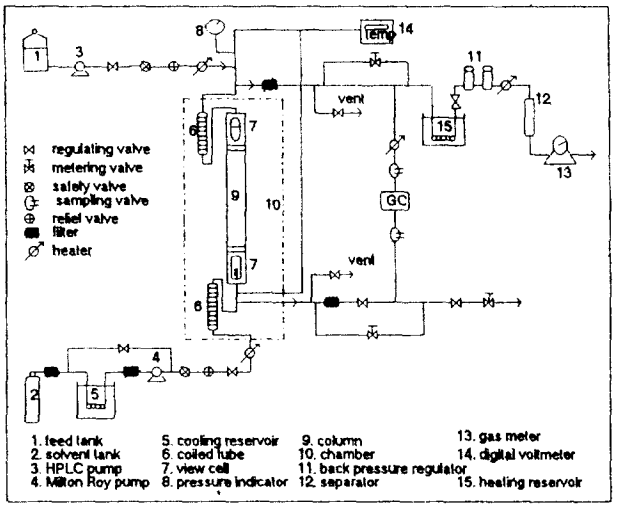

Fig. 1. Supercritical extraction apparatus.

The high pressure pumps were calibrated individually at column operating pressure, to assist in setting solvent and feed flow rates. Liquid carbon dioxide has appreciable compressibility within about 40°C of the critical, thus to ensure reliable and uniform flow from the pump, the inlet and solvent were cooled. This further ensured adequate net positive suction head (NPSH). The gaseous carbon dioxide flow was measured by a dry gas meter.

High pressure (HPLC-type) sampling valves in both lines were used to place 0.5 μl samples directly onto a gas chromatography column. Porapak-T packing column equipped with a thermal conductivity detector was sensitive to all components of the mixture with sufficient precision and accuracy for the purpose.

The purity of reagents used was food degree (99.8%) for CO_2, absolute alcohol (99.9%) and HPLC degree (AnalaR 99.7%) for iso-propanol.

The components in the extract and raffinate streams were determined by on-line gas chromatography. Peak areas were reproducible to within 3.5%. Reliability of measurement was estimated to be ±5%.

2. Procedure

Before each run, alcohol solutions were prepared and degassed by vacuum filtration. The constant temperature air chamber and pre-heating water bath were set to the desired temperature and CO_2 pump inlet chiller maintained around −20°C.

At start-up, pressure was established by carefully opening a CO_2 cylinder valve and allowing the system to reach the cylinder pressure. The column was then filled with aqueous phase by its feed pump. When the level of this phase reached the middle of the upper view cell, the interface level was maintained by the metering valve in the raffinate stream. The CO_2 pump was then started to establish the column pressure. Samples of exit streams were taken for analysis at approximately 10 minute intervals. Stream flow rates were checked every 15 minutes. For most runs, steady state was achieved within 60 minutes.

At the conclusion of each run the dispersed phase hold-up was determined by the shut-off method [Chun, 1994] in which the flow of solvent was suddenly stopped and the fall in the interface was measured when the swarm of droplets creased. Drop size was determined by photographing through the view cells and measurement by a microscope and CUE SERIES image analyser [Chun, 1994].

RESULTS AND DISCUSSION

1. Fractional Solute Recovery

Figs. 2 and 3 illustrate the fractional recovery of solute or the relative amount of solute removed by the solvent carbon dioxide from the mixture. In Fig. 2, the fractional recovery of the solute, iso-propanol (IPA) approached 80% at solvent to feed ratios above 4 for most of the experimental conditions. This includes the near critical liquid and the supercritical fluid regions. However, at 35°C and 8.27 MPa the solute recovery was low because the density of the solvent at that condition was also low at 560 kg/m^3 ($\rho_{r,CO2} = 1.195$), which, being in the retrograde region, resulted in weak solvation.

As shown in Fig. 3, it was necessary for the solvent to feed

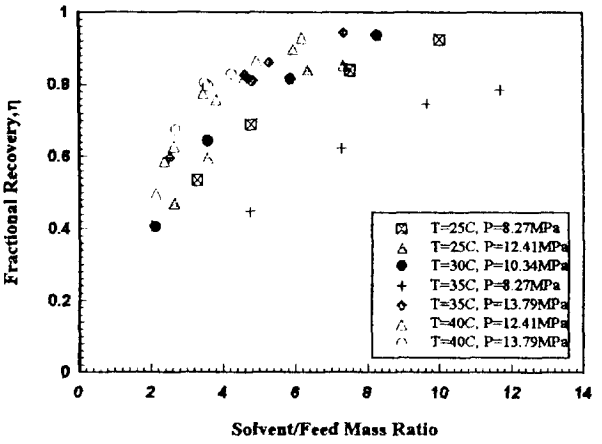

Fig. 2. Solute recovery for the system: 5 vol% IPA-water-CO_2.

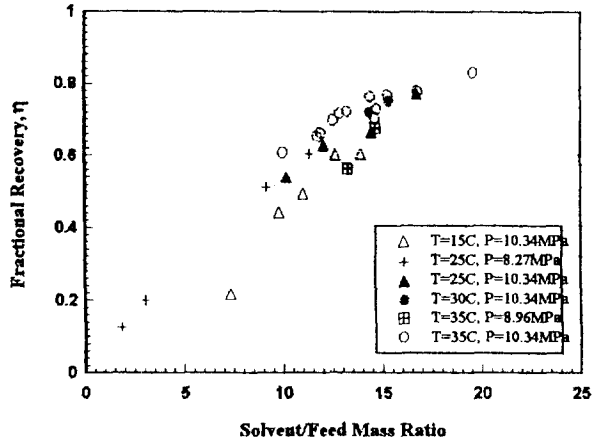

Fig. 3. Solute recovery for the system: 10 vol% EtOH-water-CO_2.

ratio to be increased to achieve 80% recovery of the solute, ethanol (EtOH). This results from the low distribution coefficient of ethanol compared with iso-propanol. At 15°C and 10.3 MPa the density increased to 866 kg/m^3 ($\rho_{r,CO2} = 0.444$) and the solvent recovered its efficiency.

2. Effect of Solvent Flow Rate on Overall Mass Transfer Coefficient

Figs. 4 and 5 show an equilibrium curve by altering the feed compositions for different runs to confirm the equilibrium data available in the literature and give good agreement with published data.

The effect of solvent flow rate on overall mass transfer coefficient K_{oc} a is shown in Fig. 6 as K_{oc} a versus the dispersed phase superficial velocity at various conditions near the supercritical region. The mass transfer efficiency was increased by increasing the solvent flow rate. This is due to increased slip velocity and dispersed phase hold-up.

Seibert and Moosberg [1988] obtained similar results in normal liquid-liquid extraction. Fig. 7 gives a comparison of the overall mass transfer coefficient for iso-propanol and ethanol systems. The mass transfer efficiency of the ethanol system is lower than that of iso-propanol due to its lower distribution coefficient.

When a solute, alcohol, is extracted from a carrier, water, by solvent, CO_2, small amounts of the water are distributed into

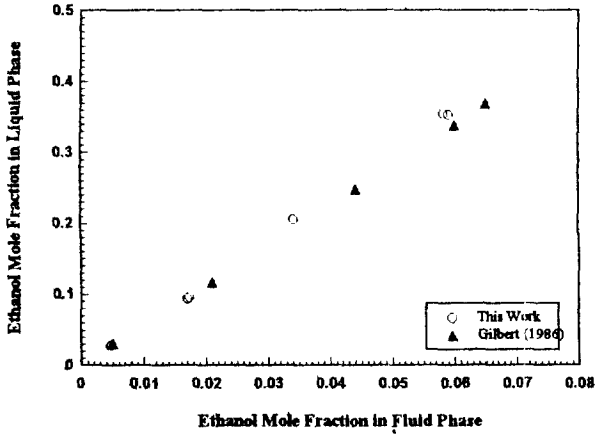

Fig. 4. Equilibrium data for the system: EtOH-water-CO_2 (T = 35°C, P = 10.3 MPa).

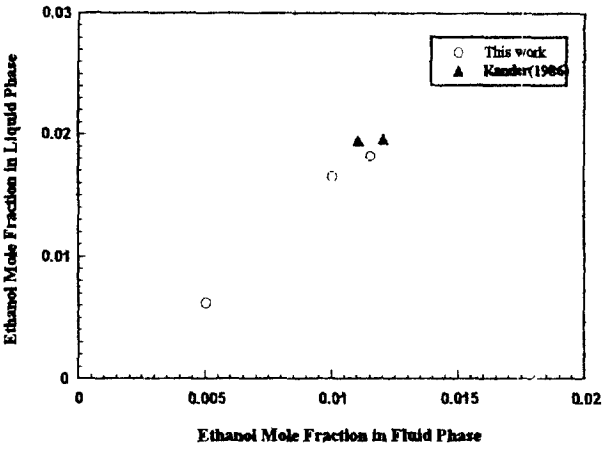

Fig. 5. Equilibrium data for the system: IPA-water-CO_2 (T = 40°C, P = 10.3 MPa).

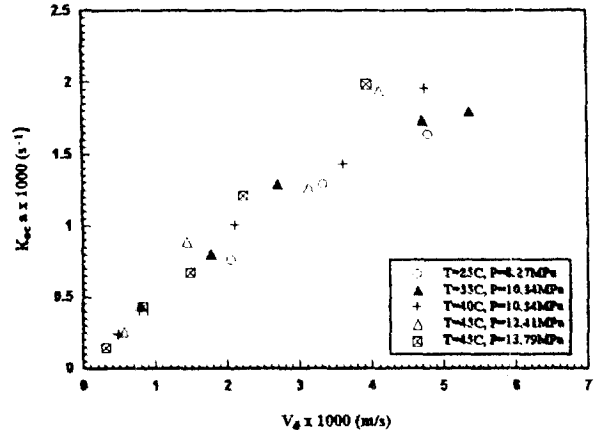

Fig. 6. Overall mass transfer coefficient vs. solvent flow rate: 10 vol% IPA-water-CO_2, $V_c = 0.4459 \times 10^{-3}$ m/s.

the solvent as well. The distribution coefficients of the solute were measured from the following equation.

$$m_s = \frac{\text{mass conc. of alcohol in solvent phase}}{\text{mass conc. of alcohol in aqueous phase}}$$

For the systems of 5 and 10 vol% IPA-water-CO_2, and 10 vol% EtOH-water-CO_2, distribution data obtained from above equation were listed in Table 1, 2 and 3 respectively.

Table 1. Distribution coefficient data for the system: 5 vol% IPA-water-CO_2

P (MPa)	T (°C)	Dense CO_2 phase y_{IPA} (-)	y_{H_2O} (-)	y_{CO_2} (-)	Aqueous phase x_{IPA} (-)	x_{H_2O} (-)	x_{CO_2} (-)	m_s (-)
8.27	25	0.0044	0.0037	0.9919	0.0089	0.9730	0.0181	0.211
12.41	25	0.0042	0.0037	0.9921	0.0079	0.9590	0.0332	0.231
10.34	30	0.0049	0.0046	0.9905	0.0093	0.9615	0.0293	0.230
12.41	30	0.0057	0.0037	0.9906	0.0091	0.9648	0.0261	0.270
8.27	35	0.0022	0.0174	0.9804	0.0107	0.9725	0.0168	0.089
10.34	35	0.0051	0.0071	0.9878	0.0082	0.9728	0.0190	0.267
12.41	35	0.0047	0.0045	0.9908	0.0068	0.9709	0.0223	0.294
13.79	35	0.0058	0.0045	0.9897	0.008	0.9704	0.0216	0.315
10.34	40	0.0042	0.0059	0.9889	0.0072	0.9727	0.0201	0.287
12.41	40	0.0051	0.0080	0.9870	0.0071	0.9726	0.0203	0.304
13.79	40	0.0084	0.0061	0.9855	0.0104	0.9672	0.0224	0.348

Table 2. Distribution coefficient data for the system: 10 vol% IPA-water-CO_2

P (MPa)	T (°C)	Light phase y_{IPA} (-)	y_{H_2O} (-)	y_{CO_2} (-)	Heavy phase x_{IPA} (-)	x_{H_2O} (-)	x_{CO_2} (-)	m_s (-)
8.27	25	0.0092	0.0057	0.9851	0.0172	0.9634	0.0194	0.235
10.34	25	0.0112	0.0038	0.9850	0.0197	0.9586	0.0217	0.251
12.41	25	0.0104	0.0046	0.9850	0.0178	0.9551	0.0271	0.260
13.79	25	0.0100	0.0042	0.9858	0.0173	0.9554	0.0273	0.254
10.34	30	0.0112	0.0048	0.9840	0.0193	0.9590	0.0217	0.256
8.27	35	0.0048	0.0210	0.9742	0.0228	0.9601	0.0171	0.093
10.34	35	0.0106	0.0066	0.9828	0.0163	0.9632	0.0206	0.286
12.41	35	0.0126	0.0055	0.9819	0.0180	0.9598	0.0222	0.308
13.79	35	0.0113	0.0062	0.9825	0.0151	0.9598	0.0232	0.328
10.34	40	0.0116	0.0083	0.9800	0.0185	0.9617	0.0219	0.277
12.41	40	0.0144	0.0081	0.9774	0.0186	0.9596	0.0202	0.341

Table 3. Distribution coefficient data for the system: 10 vol% EtOH-water-CO_2

P (MPa)	T (°C)	Light phase y_{IPA} (-)	y_{H_2O} (-)	y_{CO_2} (-)	Heavy phase x_{IPA} (-)	x_{H_2O} (-)	x_{CO_2} (-)	m_s (-)
10.34	15	0.0029	0.0039	0.9933	0.0288	0.9328	0.0384	0.045
8.27	25	0.0039	0.0048	0.9913	0.0300	0.9414	0.0286	0.058
10.34	25	0.0038	0.0030	0.9932	0.0274	0.9404	0.0322	0.062
10.34	30	0.0043	0.0036	0.9921	0.0285	0.9411	0.0305	0.068
6.89	35	0.0020	0.0155	0.9824	0.0304	0.9486	0.0210	0.030
8.96	35	0.0028	0.0054	0.9918	0.0285	0.9455	0.0260	0.043
10.34	35	0.0047	0.0052	0.9901	0.0282	0.9470	0.0248	0.073

3. Effect of Temperature and Pressure on Overall Mass Transfer Coefficient

Fig. 8 shows the effects of temperature and the dispersed phase superficial velocity on the overall mass transfer coefficient at constant continuous phase superficial velocity for the 5 vol% IPA-water-carbon dioxide. This figure demonstrates that with increasing solvent flow rates, both the near critical liquid and supercritical fluid show steadily increasing mass transfer efficiency.

Fig. 9 shows the effect of pressure on the overall mass transfer coefficient. Here the dispersed phase superficial velocity

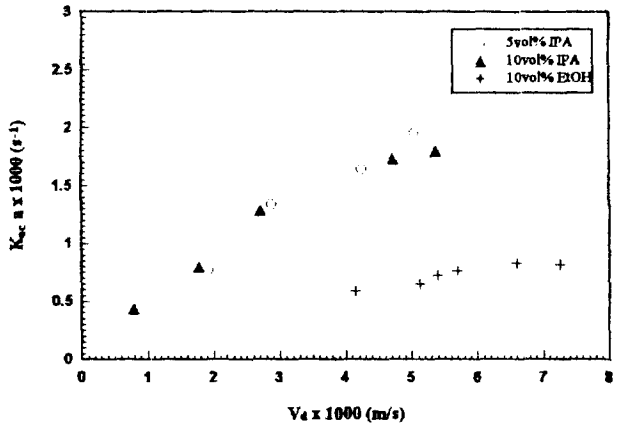

Fig. 7. Overall mass transfer coefficient comparison: Vc=0.4459 $\times 10^{-3}$ m/s T = 35°C, P = 10.3 MPa.

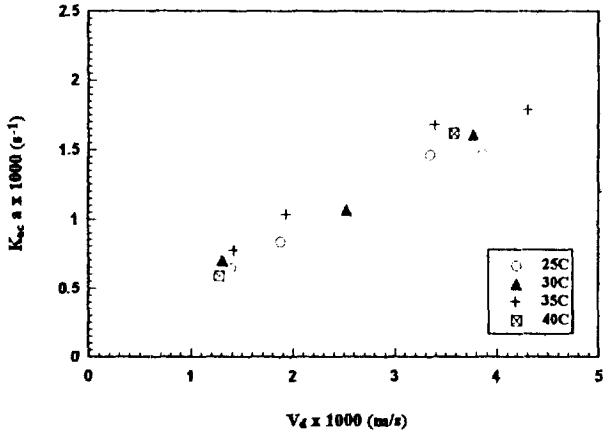

Fig. 8. Effect of temperature on K_{oc} a: 5 vol% IPA-water-CO_2, P = 12.41 MPa Vc = 0.4459 $\times 10^{-3}$ m/s.

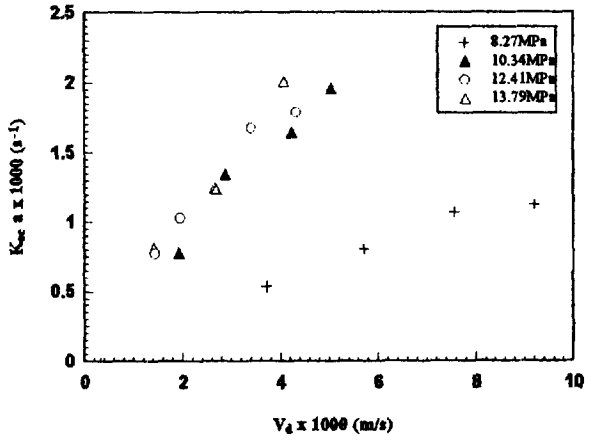

Fig. 9. Effect of pressure on K_{oc} a: 5 vol% IPA-water-CO_2, Vc = 0.4459 $\times 10^{-3}$ m/s T = 35°C.

changes at constant continuous phase superficial velocity and temperature. In both near-critical and supercritical regions the overall mass transfer coefficient increased constantly with increased dispersed phase velocity. However, the overall mass transfer coefficient at 8.27 MPa (solvent density = 560.1 kg/m^3) was smaller due to the low distribution coefficient (m_s = 0.089) and weak concentration driving force.

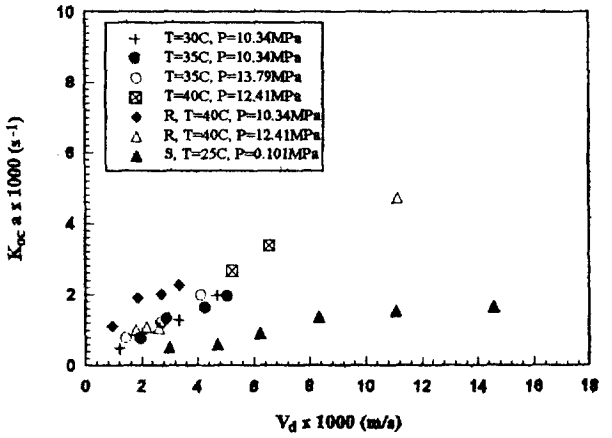

Fig. 10. Comparison of K_{oc} a between supercritical and conventional systems: This work: IPA-water-CO_2, R: Rathkamp et al. [1987] IPA-water-CO_2, S: Seibert and Moosberg [1988] acetone-water-toluene.

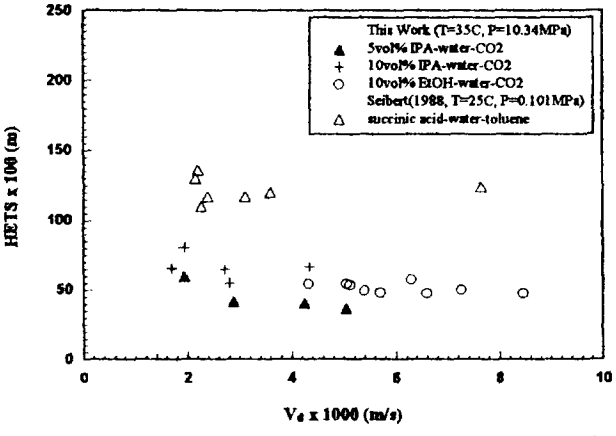

Fig. 11. Comparison of column efficiency between supercritical and conventional systems.

4. Mass Transfer Comparison between Supercritical and Conventional Systems

The data obtained from this work were compared first with those of Rathkamp et al. [1987] in supercritical extraction and then with Seibert and Moosberg [1988] in conventional liquid-liquid extraction.

Figs. 10 and 11 show that enhanced mass transfer is achieved in a supercritical solvent system. These data show good agreement with Rathkamp et al. [1987].

DATA CORRELATION

1. Hold-up

The operational hold-up results are illustrated in Fig. 12. The graph shows that operational hold-up is directly dependent on the superficial velocity of the dispersed phase flow rate. A modified correlation [Idogawa et al., 1987] was obtained as the following.

$$\frac{\phi_d}{1-\phi_d} = 0.090 V_d^{0.8} \rho_d^{0.17} \left(\frac{\gamma}{72}\right)^{-0.22exp(-P)} \quad (10)$$

The experimental data plotted in Fig. 13 shows good agree-

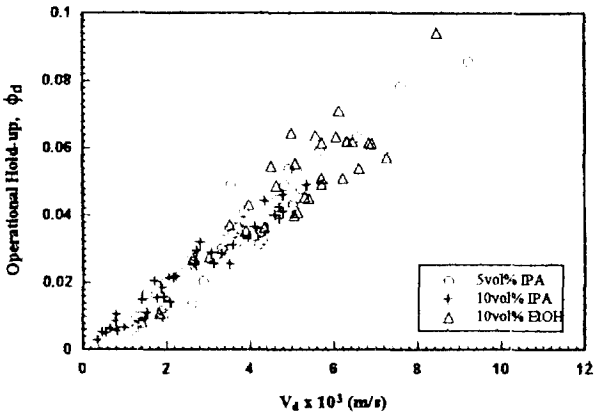

Fig. 12. Operational hold-up as function of dispersed phase superficial velocity.

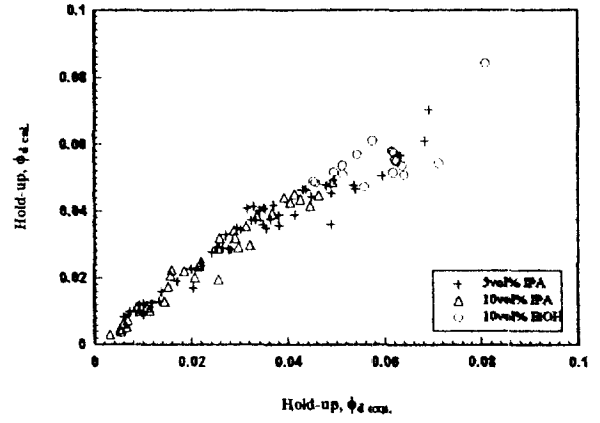

Fig. 13. Hold-up parity plot.

ment when compared with the values calculated from Eq. (10) with an A.A.R.D. of 12.4%.

2. Drop Size

Individual drop sizes were measured by analysing photographs with a CUE 3 image analyser. Experimental data obtained were correlated by the following equation based on Kumar's model [Kumar and Hartland, 1984]:

$$\frac{d_s}{N_d} = 1.909\left[\frac{\Delta\rho N_d N_v^2}{\gamma}\right]^{-0.003}\left[\frac{\Delta\rho N_v^2 g}{\gamma}\right]^{-0.146} \tag{11}$$

Fig. 14 shows the correlation of experimental data over the ranges of velocities and system conditions studied. The model for drop diameter agrees well with experimental data within an average deviation of 7.3%.

3. Individual Mass Transfer Coefficient

Internal circulation within drops can play an important role in determining the dispersed phase film coefficient. In this work, Handlos' model [Handols and Baron, 1957] was chosen based on fully developed circulation in the drop.

$$k_d = 0.00375 V_s\left(\frac{\mu_c}{\mu_c+\mu_d}\right) \tag{12}$$

Slip velocity, V_s, is expressed as a function of the dispersed phase hold-up, ϕ_d, which is meant with the volume fraction of

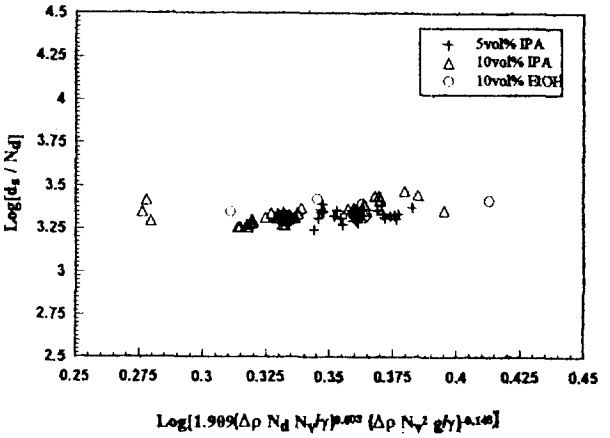

Fig. 14. Correlation of drop size in spray columns.

the solvent-feed mixture in the column occupied by the solvent and the superficial velocities, V_c and V_d, of feed and solvent.

$$V_s = \frac{V_d}{\phi_d} + \frac{V_c}{1-\phi_d} \tag{13}$$

In Eq. (12) the viscosities were obtained from the table of Ulybin and Makarushkin [1977].

Individual mass transfer coefficients in the countercurrent extraction column were not measured due to the complexity of the flow conditions. But the overall coefficient can be obtained from Eq. (3). Dimensional analysis may be used to relate the film mass transfer coefficient to the dimensionless groups, Schmidt number, Reynolds number, Capillary number, with some assumed degree of mixing or turbulence in the continuous phase in the wake of a bubble or drop:

$$Sh_c = A_1 Sc_c^{A2}\, Re^{A3}\, Ca^{A4}(1-\phi_d) \tag{14}$$

In dimensionless group, the densities of carbon dioxide were obtained from the IUPAC tables [Angues et al., 1976] interpolated using the Peng-Robinson [1976] equation of state and diffusivities were measured from Wilke-Chang [1955] equation. Interfacial tension was measured experimentally [Chun, 1994]. The ranges of values of dimensionless numbers used in this work are: 330<Re_c<870, 315<Sc_c<985, 6<Ca<9. The constants A_1, A_2, A_3 and A_4 in Eq. (13) were obtained by least squares method.

$$Sh_c = A_1 Sc_c^{0.606} Re_c^{0.369} Ca^{-0.007}(1-\phi_d) \tag{15}$$

The values of constant A_1 in Eq. (14) are listed in Table 1 for different conditions.

Fig. 15 is a parity plot of the values calculated from Eq. (3) versus the experimental from Eq. (6). Experimental data agree well with the models with A.A.R.D. of 11.76 and 11.23 % respectively.

CONCLUSION

Mass transfer to carbon dioxide in near- and supercritical conditions for the systems iso-propanol and ethanol with water in a countercurrent spray column has been investigated and analysed with the aid of Withman's two-film model. The mass

Table 4. Values of constant A_i in Eq. (15) regressed from experimental data

System	Condition	Value (A_i)
5 vol% *IPA-W-C	lower m_s gas-like CO_2	0.0521
	higher m_s liquid-like CO_2	0.2654
10 vol% *IPA-W-C	higher m_s liquid-like CO_2	0.2057
10 vol% **EtOH-W-C	lower m_s gas- and liquid-like CO_2	0.0653

*IPA-W-C: iso-propanol-water-CO_2
**EtOH-W-C: ethanol-water-CO_2

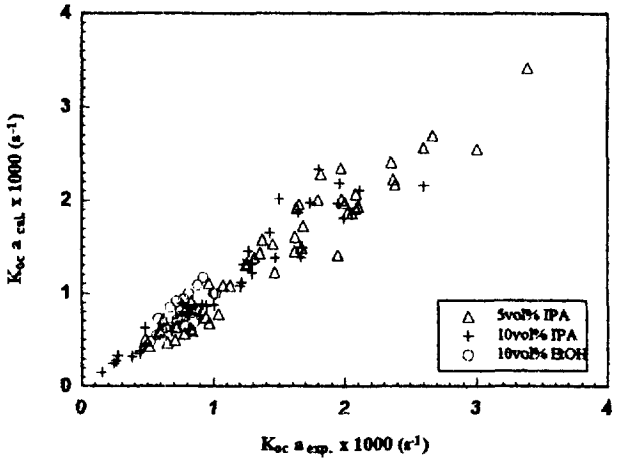

Fig. 15. Overall mass transfer coefficient parity plot.

transfer efficiency of supercritical carbon dioxide has been shown to be more than twice that of conventional liquid-liquid extraction. Moreover, the less dense carbon dioxide, due to its weak solvating ability and gas-like density, gave low mass transfer efficiencies. Changes in the physical properties of density, viscosity, diffusivity and distribution coefficient, were largely responsible for the enhanced mass transfer rate.

Recovery of iso-propanol was 30% higher than ethanol due to its higher distribution coefficient and larger slip velocity. At the vicinity of the critical point the less dense carbon dioxide produced low solute extraction efficiency. Hold-up was found to be dependent on solvent flow rate but drop size was independent. The experimental data of the hold-up and drop-size were correlated with system properties.

A model for the continuous phase film mass transfer coefficient was developed by using dimensionless group analysis. The model demonstrated that the capillary number, involving the interfacial tension term had a slight effect on the mass transfer coefficient. However, the Schmidt number, containing the diffusivity, had a great influences on the mass transfer coefficient.

NOMENCLATURE

a : interfacial area [m^2/m^3]
A_1, A_2, A_3 and A_4 : constants defined in Eq. (13), (14) [-]
A.A.R.D. : average absolute relative deviation [-]
Ca : capillary number, $d_s^2 \rho_c g/\gamma$ [-]
d_s : mean drop diameter [m]
D : molecular diffusivity [m^2/s]
F : solute flux [m/hr]
g : gravitational constant [9.8 m/s^2]
H : effective column height [m]
HTU : height of a transfer unit [m]
HETS : height equivalent of theoretical stage [m]
k : film mass transfer coefficient [m/s]
K : overall mass transfer coefficient [m/s]
m_s : distribution coefficient of alcohol based on a mass concentration driving force [-]
N_d : diameter of nozzle [m]
N_v : velocity at nozzle [m/s]
NTU_{oc} : number of transfer units [-]
Re : Reynolds number [$(\rho V_s d_s)/\mu$]
S/F : mass ratio of solvent to feed [-]
Sc : Schmidt number [$\mu(\rho/D)$]
Sh : Sherwood number [$k d_s/D$]
V : superficial velocity [m/s]
V_s : slip velocity [m/s]
x : mole fraction of solute in liquid phase [-]
y : mole fraction of solute in vapour phase [-]

Greek Letters

β : extraction factor
ε : void fraction [-]
ϕ_d : operational hold-up [-]
γ : interfacial tension [$mN \cdot m^{-1}$]
η : fractional recovery [-]
μ : viscosity [N sec./m^2]
ρ : density [$kg \cdot m^{-3}$]
$\Delta\rho$: density difference [kg/m^3]

Subscripts

c : continuous phase; critical
d : dispersed phase
e : extraction stream
EtOH : ethanol
g : gas
IPA : iso-propanol
oc, od : overall, based on continuous and dispersed phases, respectively
r : raffinate stream
s : solute, alcohol

Superscript

* : equilibrium conditions

REFERENCES

Angus, S., Armstrong, B. and de Reuck, K. M., "IUPAC International Tables of the Fluid State-Carbon Dioxide", Pergamon Press, New York, 1976.

Brunner, G. and Kreim, K., "Separation of Ethanol from Aqueous Solutions by Gas Extraction", *Ger. Chem. Eng.*, **9**, 246 (1986).

Chun, B. S., "Mass Transfer and Hydrodynamic Behavior of

Spray and Packed Columns in Supercritical Fluid Extraction", Ph.D Dissertation, Univ. of South Australia, Australia (1994).

Handlos, A. E. and Baron, T., "Mass Transfer from Drops in Liquid-Liquid Extraction", *AIChE J.*, **3**, 127 (1957).

Higbie, R., "The Rate of Absorption of a Pure Gas into a Still Liquid during Short Periods of Exposure", *Trans. Amer. Inst. Chem. Engnr.*, **May 13**, 365 (1935).

Idogawa, K., Ikeda, K., Fukuda, T. and Morooka, S., "Effect of Gas and Liquid Properties on the Behavior of Bubbles in a Column under High Pressure", *Int. Chem. Eng.*, **27**, 93 (1987).

Johnson, A. I. and Hamielec, A. E., "Mass Transfer Inside Drops", *AIChE J.*, **6**, 145 (1960).

Kumar, A. and Hartland, S., "Correlation for Drop Size in Liquid/Liquid Spray Columns", *Chem. Eng. Commun.*, **31**, 193 (1984).

Lahiere, R. J. and Fair, J. L., "Mass Transfer Efficiencies of Column Contactor in Supercritical Critical Extraction Service", *Ind. Eng. Chem. Res.*, **26**, 2086 (1987).

Peng, D. Y. and Robinson, D. B., "A New Two-Constant Equation of State", *Ind. Eng. Chem. Fundam.*, **15**(1), 59 (1976).

Pratt, H. R. C., "Liquid-Liquid Extraction in Theory and Practice", *Ind. Chem.*, Feb. 63 (1955).

Rathkamp, P. J., Bravo, J. L. and Fair, J. R., "Evaluation of Packed Columns in Supercritical Extraction Processes", *Solv. Extr. & Ion Exch.*, **5**, 3676 (1987).

Ruby, C. L. and Elgin, J. C., "Mass Transfer between Liquid Drops and a Continuous Liquid Phase in a Countercurrent Fluidized System: Liquid-Liquid Extraction in a Spray Tower", *Chem. Eng. Progr., Symp., Ser.*, **51**(16), 17 (1955).

Seibert, A. F. and Moosberg, D. G., "Performance of Spray, Sieve Tray and Packed Contactors for High Pressure Extraction", *Sep. Sci. Tech.*, **23**, 2049 (1988).

Skelland, A. H. P. and Huang, Y.-F., "Dispersed Phase Mass Transfer during Drop Formation under Jetting Conditions", *AIChE J.*, **25**, 80 (1979).

Thornton, J. D., "Science and Practice of Liquid-Liquid Extraction vol.1 and 2", Oxford Eng. Sci. Series 27, 1992.

Treybal, R. E., "Mass Transfer Operations", 3rd ed, McGraw-Hill, New York, NY (1980).

Ulybin, S. A., Makarushkin, W. I., "The Viscosity of Carbon Dioxide at 220-1300 K and Pressures up to 300 MPa", *Proc. Sym. Thermophys. Prop.*, **7**, 768 (1977).

Whitman, W. G., "The Two-Film Theory of Gas Absorption", *Chem. and Metal. Eng.*, **29**, 146 (1923).

Wilke, C. R. and Chang, P., "Correlation of Diffusion Coefficients in Dilute Solutions", *AIChE J.*, **1**, 264 (1955).